The Successive-Order-of-Interaction Radiative Transfer Model. Part I: Model Development

ANDREW K. HEIDINGER

Advanced Satellite Products Branch, NOAA/NESDIS Office of Research and Applications, Madison, Wisconsin

CHRISTOPHER O'DELL AND RALF BENNARTZ

Department of Atmospheric and Oceanic Sciences, University of Wisconsin—Madison, Madison, Wisconsin

THOMAS GREENWALD

Cooperative Institute for Meteorological Satellite Studies, University of Wisconsin—Madison, Madison, Wisconsin

(Manuscript received 9 March 2005, in final form 22 October 2005)

ABSTRACT

This study, the first part of a two-part series, develops the method of "successive orders of interaction" (SOI) for a computationally efficient and accurate solution for radiative transfer in the microwave spectral region. The SOI method is an iterative approximation to the traditional adding and doubling method for radiative transfer. Results indicate that the approximations made in the SOI method are accurate for atmospheric layers with scattering properties typical of those in the infrared and microwave regions. In addition, an acceleration technique is demonstrated that extends the applicability of the SOI approach to atmospheres with greater amounts of scattering. A comparison of the SOI model with a full Monte Carlo model using the atmospheric profiles given by Smith et al. was used to determine the optimal parameters for the simulation of microwave top-of-atmosphere radiances. This analysis indicated that a four-stream model with a maximum initial-layer optical thickness of approximately 0.01 was optimal. In the second part of this series, the accuracies of the SOI model and its adjoint are demonstrated over a wide range of microwave remote sensing scenarios.

1. Introduction

Difficulties in the accurate and rapid simulation of radiation that is multiply scattered have limited the use of satellite infrared and microwave observations in cloudy regions for data assimilation in numerical weather prediction (NWP) schemes. This paper presents a technique that allows for computationally efficient modeling of azimuthally symmetric radiative transfer in moderately scattering atmospheres. Azimuthally symmetric radiation refers to radiation that has no dependence on azimuth as is the case in the microwave and infrared regions where the contribution from the solar beam is negligible. The inclusion of the solar beam, however, is straightforward but is not described here because the specific goal for this technique is to be accurate for most cloudy and precipitating atmospheres in the infrared and microwave spectral regions. The method developed here is dubbed the "successive order of interactions" (SOI) and involves a mix of analytic and iterative methods. This paper explains the method, determines its accuracy for a wide range of conditions, and demonstrates its application to the simulation of satellite microwave observations. In the second part of this series (O'Dell et al. 2006, hereinafter referred to as Part II), the application of this model to the simulation of microwave radiances is described and tested over a wide range of atmospheric conditions.

The most common approach for the rapid simulation of microwave observations in cloudy atmospheres is the delta-Eddington two-stream method (Bauer et al. 2004). For example, Liu and Weng (2002) recently developed a two-stream model that included polarization

Corresponding author address: Andrew K. Heidinger, NOAA/NESDIS Office of Research and Applications, 1225 West Dayton, Madison, WI 53706.
E-mail: andrew.heidinger@noaa.gov

for application in the microwave region. As shown later, the ability of the SOI model to include multiple (more than two) streams is an important factor in its accuracy for some remote sensing applications. The SOI model developed here shares some similarities with the approach outlined in Voronovich et al. (2004) in that both approaches employ a modified doubling approach. However, the SOI model developed here differs from Voronovich et al. in the use of an iterative approach when treating multiple layers.

2. Development of the SOI method

The SOI method draws from two traditional methods of solution of radiative transfer: the doubling technique (van de Hulst and Grossman 1968; Twomey et al. 1966; Hansen 1969) and the successive-order-of-scattering (SOS) technique (Busbridge 1960; Irvine 1965; Weinman and Guetter 1977; Wendisch and von Hoyningen-Huene 1991; Herman et al. 1995; Greenwald et al. 2005). The doubling technique, which is applied in adding and doubling models, has been successfully used in many remote sensing applications. As described later, the main problem with the doubling technique is that it can be computationally expensive for optically thick layers with significant amounts of scattering. In contrast, the SOS approach is computationally efficient only for atmospheres with limited amounts of scattering. The SOI method is an attempt to optimally combine these two methods to develop a radiative transfer model that is both computationally efficient and applicable to atmospheres in which radiation undergoes multiple scattering.

The development of the SOI model was motivated by the desire to improve the performance of the SOS model, described by Greenwald et al. (2005), in atmospheres with large amounts of scattering. The SOI model described here therefore maintains many similarities with that SOS model. For example, both the SOI and SOS approaches use an iterative method, in place of the adding approach, to integrate the radiative effects of multiple layers together. However, the largest difference between the two approaches is in the computation of the radiative properties of each layer. The SOS model requires that the model layers be optically thin enough that the single-scattering approximation is valid. As explained by Greenwald et al., this requires the SOS model to subdivide an atmosphere with large amounts of scattering into hundreds or thousands of layers. The SOI method overcomes the requirement for optically thin layers by using a modified doubling method to compute the radiative properties of layers that can be optically thick.

The SOS and SOI methods both apply an iterative approach to solve the radiative transfer equation. In both methods, each iteration implies an additional interaction of the photons that compose the desired radiative quantity with each model layer. In both methods, the first iteration or interaction is composed of the unscattered thermal emission from each layer. The difference between the two methods occurs in the subsequent interactions that involve scattering. Where the SOS model uses the single-scattering approximation to derive the radiative properties of each layer, the SOI model uses a truncated doubling approach to include multiple scattering in the computation of each layer's radiative properties. In the SOS model, each interaction is therefore restricted to be one additional order of scattering. In the SOI model, each interaction can include multiple additional orders of scattering. For this reason, we chose to differentiate the SOI model from the SOS approaches. As discussed later, one impact of the SOI's ability to allow for multiple scattering in each interaction is that the optical thickness of a model layer can be much thicker than that used in the SOS approach. In the SOS approach, each model layer's optical thickness must be thin enough such that the single scatter approximation is valid.

The goal of this paper is to demonstrate that the approximations used in the SOI model significantly extend its ability to simulate atmospheres with multiple scattering beyond that of the SOS model, while maintaining the computational efficiency required for real-time NWP applications. In the remainder of this paper, the physical basis of the SOI approach will be explained. The next sections will describe the approximations that underpin the SOI model and demonstrate their range of applicability. This paper will conclude with a comparison of the SOI model results with those from a Monte Carlo model. This comparison is used to select the SOI model parameters for optimal performance for microwave remote sensing. Part II will further demonstrate the accuracy of the SOI model and its adjoint for the simulation and assimilation of microwave observations.

a. Truncation of the doubling method

The first step in the SOI model is to compute the radiative properties for each model layer. The computation of these layer properties involves one of the main approximations used in the SOI model: the truncated doubling approximation. The method of doubling to compute the radiative properties of a layer is well established (Wiscombe 1975a,b). Given an arbitrarily thin initial layer, doubling has been demonstrated to produce accurate and numerically stable results for any

range of optical properties and for layers of any optical thickness.

The doubling method is an application of the adding method when the two layers being added are identical. For reference, the doubling method is briefly described and, except for the truncation approximation described below, the application of doubling in the SOI model is a standard implementation. Given the reflectance $\mathbf{R}_h$ and the transmittance $\mathbf{T}_h$ matrices for a layer with one-half of the optical thickness of the final layer, the reflectance $\mathbf{R}$ of the final layer can be computed as

$$\mathbf{R} = \mathbf{T}_h\mathbf{\Gamma}\mathbf{R}_h\mathbf{T}_h + \mathbf{R}_h, \tag{1}$$

and the transmittance of the final layer $\mathbf{T}$ can be computed as

$$\mathbf{T} = \mathbf{T}_h\mathbf{\Gamma}\mathbf{T}_h. \tag{2}$$

The matrix $\mathbf{\Gamma}$ is defined as

$$\mathbf{\Gamma} = (\mathbf{E} - \mathbf{R}_h\mathbf{R}_h)^{-1}, \tag{3}$$

where $\mathbf{E}$ is the identity matrix; $\mathbf{\Gamma}$ physically represents the higher-order reflections between the two adjacent layers being added together to perform a doubling step. The matrices $\mathbf{R}$, $\mathbf{T}$, and $\mathbf{\Gamma}$ are square matrices dimensioned by the number of streams simulated per hemisphere. Using the notation of Wiscombe (1975b), the source exiting the top of the layer $\mathbf{S}^+$ and the source exiting the bottom of the layer $\mathbf{S}^-$ are defined as

$$\mathbf{S}^+ = \frac{B_o + B_n}{2}\mathbf{Y} + \frac{(B_o - B_n)}{\delta\tau}\mathbf{Z} \quad \text{and} \tag{4}$$

$$\mathbf{S}^- = \frac{B_o + B_n}{2}\mathbf{Y} - \frac{(B_o - B_n)}{\delta\tau}\mathbf{Z}, \tag{5}$$

where B_o is the blackbody emission at the top of the layer, B_n is the blackbody emission at the base of the layer, and $\delta\tau$ is the layer optical thickness. Note that $\mathbf{S}^+$, $\mathbf{S}^-$, $\mathbf{Y}$, and $\mathbf{Z}$ are vectors dimensioned by the number of streams. As described by Wiscombe (1975a), $\mathbf{Y}$ is the vector determining the thermal source from an isothermal layer and $\mathbf{Z}$ is the term that accounts for a linear variation of emission through the layer. The doubling rule for $\mathbf{Y}$ is

$$\mathbf{Y} = (\mathbf{T}_h\mathbf{\Gamma} + \mathbf{T}_h\mathbf{\Gamma}\mathbf{R}_h + \mathbf{E})\mathbf{Y}_h, \tag{6}$$

and the doubling rule for $\mathbf{Z}$ is

$$\mathbf{Z} = \mathbf{Z}_h + g_h\mathbf{Y}_h + (\mathbf{T}_h\mathbf{\Gamma} - \mathbf{T}_h\mathbf{\Gamma}\mathbf{R}_h)(\mathbf{Z}_h - g_h\mathbf{Y}_h), \tag{7}$$

where g_h is a scalar term that is doubled with each doubling step.

In the above expressions, the matrix $\mathbf{\Gamma}$ appears several times and is the quantity requiring a matrix inversion. Therefore, the computational cost of the doubling technique would be reduced if these matrix inversions could be eliminated. Therefore, in the SOI model, $\mathbf{\Gamma}$ is approximated using Taylor's rule for expanding infinite series, which allows the above expression to be approximated as follows:

$$\mathbf{\Gamma} = \mathbf{E} + \mathbf{R}_h\mathbf{R}_h + [(\mathbf{R}_h\mathbf{R}_h)^2], \tag{8}$$

where up to two terms in the series expansion of $\mathbf{\Gamma}$ have been retained. Because the higher-order terms have been ignored or truncated in the computation of $\mathbf{\Gamma}$, the method of doubling using (8) is referred to here as truncated doubling. In practice, the SOI model chooses when to apply the one- or two-term expansion, and this logic is explained later.

To test the accuracy of the truncated doubling method, comparisons were made of single-layer results using the full doubling procedure and the truncated doubling procedure using either one or two terms in the expansion of $\mathbf{\Gamma}$. As described later, the SOI model determined to be optimal for the simulation of microwave radiances was the four-stream model with an initial-layer optical thickness of 0.01, and this default configuration will be used for all of the simulations. In the default SOI model, an additional stream was inserted at a specified zenith angle to avoid the need to interpolate from the quadrature points (Evans and Stephens 1990). For these simulations the additional quadrature point is at a zenith angle of 30°. This additional quadrature point is given a weight of zero and contributes nothing to the actual solution at the original quadrature points. This model is therefore still a four-stream model and will be referred to as a 4 + 2–stream model. For low numbers of streams, inclusion of an additional stream was found to be more accurate than interpolating from the actual quadrature points. The disadvantage is the extra computational cost of a larger dimension in each matrix and vector in the doubling process. This model is designed for both infrared and microwave applications, but for simplicity the Rayleigh–Jeans approximation is used throughout this paper and the units of all radiance terms will be kelvins.

Figure 1 shows the errors resulting from the truncated doubling approximation for the upwelling emission from an isothermal cloud with a temperature of 285 K viewed with a zenith angle of 30°. The method of initialization used (described later) is the exponential infinitesimal generator initialization method with an initial optical thickness of 0.01. The left-hand plot shows the actual variation in the upwelling brightness temperature T_b at the top of the cloud as a function of layer optical depth and single-scattering albedo. As the cloud becomes optically thicker and more absorbing, the emissivity of the cloud increases and the observed

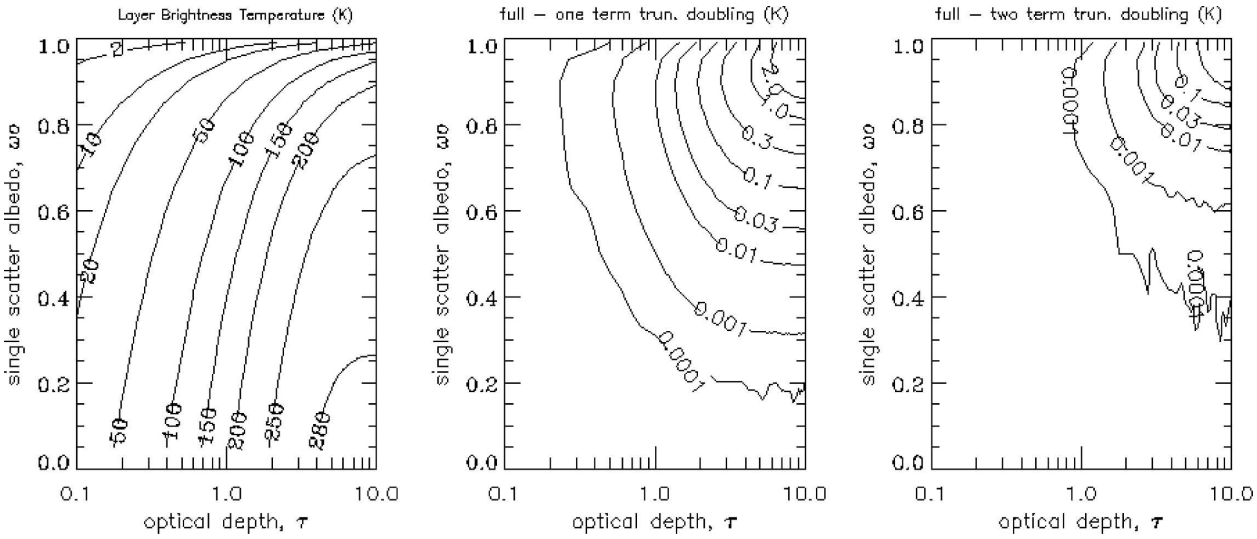

FIG. 1. Errors in the emission from a single layer resulting from the truncation of the doubling as function of the layer optical thickness τ and single-scattering albedo $\tilde{\omega}$. These computations were made using an HG phase function with $g = 0.6$ and a viewing angle of 30° using the default SOI model. (left)The actual variation in top-of-atmosphere brightness temperature using the full doubling method. (middle) The difference between the full and one-term-truncated doubling. (right) The difference between the full and the two-term doubling.

T_b approaches the cloud temperature. The center plot shows the difference in radiance when the full expression for $\mathbf{\Gamma}$ is used in the doubling versus when the single-term expansion is used. The right-hand plot shows the difference between the full doubling and the two-term expansion for $\mathbf{\Gamma}$. The results indicate that the single-term expansion is adequate for most of the $\tau - \tilde{\omega}$ space except for the most optically thick ($\tau > 4$) and least absorbing ($\tilde{\omega} > 0.8$) region. For this region, the single-term approximation can cause errors exceeding 2 K. However, the use of the two-term approximation greatly reduces the errors in this region. For most of the optical conditions characteristic of microwave and infrared radiative transfer, the single-term approximation results in errors much less than 0.1 K.

Note that, when running the SOI model with a low number of streams, the computational benefit of the truncated doubling is not necessary because the matrix inversion given in (3) can be computed simply without the use of a generic matrix inversion routine. However, for many applications, the accurate simulation of radiance requires more than four streams. In these applications, the use of the truncated doubling as described above is critical to allowing the SOI model to meet the computational requirements for real-time data assimilation.

b. Initial-layer calculations

As described above, the truncated doubling approximation can accurately compute the radiative quantities ($\mathbf{R}$, $\mathbf{T}$, $\mathbf{S}^{\pm}$) for a single layer while avoiding matrix inversions. The actual accuracy of final radiative quantities also depends on the values of the initial radiative quantities of the thin layer used to initialize the doubling procedure. The radiative quantities produced from the initialization method are related to the reflectance and transmittance matrices for the initial layer ($\mathbf{R}_o$ and $\mathbf{T}_o$) as well as $\mathbf{Y}_o$, the initial-layer thermal source vector. The values of $\mathbf{R}_o$, $\mathbf{T}_o$, and $\mathbf{Y}_o$ are used as the initial values for $\mathbf{R}_h$, $\mathbf{T}_h$, and $\mathbf{Y}_h$ in (1)–(3) and (6) to begin the doubling process. The goal here is to select an initialization method that optimizes speed while maintaining sufficient accuracy for the SOI method. This section describes the method chosen for the initial-layer calculations and the sensitivity of the results to this method.

The work of Wiscombe (1975b) examines various choices for the doubling initialization. For convenience in the discussion to follow, the following terms are defined that appear repeatedly in the description of the initialization methods. These terms describe the local reflectance r and transmittance t and are functions of only the single-scattering properties of the medium. The local reflectance matrix $\mathbf{r}$ is defined here as

$$r_{ij} = 0.5\tilde{\omega}P_{ij}^{-}w_j, \tag{9}$$

and the local transmission matrix $\mathbf{t}_l$ is defined as

$$t_{ij} = 0.5\tilde{\omega}P_{ij}^{+}w_j. \tag{10}$$

In the above expressions $\tilde{\omega}$ is the single-scattering al-

bedo and $\mathbf{P}^+$ ($\mathbf{P}^-$) is the scattering phase function matrix for forward (backward) scattering; i represents the emergent direction, and j is the incident direction. For convenience, we have included the quadrature weight w in this definition. The details of the quadrature scheme and the handling of the phase function in the SOI model are identical to those in the SOS model of Greenwald et al. (2005). The phase function used in the SOI model is a Henyey–Greenstein (HG) representation. The actual incorporation in the SOI model uses a Legendre expansion of the azimuthally averaged phase function. As discussed in the SOS model description, delta scaling was found to offer little benefit in the microwave simulations shown here and was not used, but it was included as an option in the model.

The work of Wiscombe (1975b) examines various initialization schemes in detail. His analyses were focused on the applicability to the true doubling method, and computational efficiency was not a driving issue. In general, the many initialization methods all assume that the initial layers are sufficiently thin such that various thin-layer approximations apply. One method for computing the radiative quantities for the initial layer is to apply directly the full single-scattering approximation, which assumes that the layer is sufficiently optically thin that radiation passing the through layer experiences at most one scattering event. This single-scattering initialization (SSI) can be derived from direct application of the single-scattering radiative transfer equation (Liou 2002) or from the doubling formulas themselves where only terms $O(\tilde{\omega})$ are retained (Wiscombe 1975b). With this approximation, the initial-layer reflectance matrix for the single-scattering initialization is defined as

$$R_{ij}^{\mathrm{ssi}} = r_{ij}\frac{1 - e^{-m_{ij}\delta\tau}}{m_{ij}\mu_i}, \tag{11}$$

and the initial layer transmittance for the SSI is

$$T_{ij}^{\mathrm{ssi}} = e^{-\delta\tau/\mu_i}t_{ij}\frac{1 - e^{-n_{ij}\delta\tau}}{n_{ij}\mu_i} + E_{ij}e^{-\delta\tau/\mu_i}, \tag{12}$$

where $\mathbf{E}$ is the identity matrix and $\delta\tau$ represents the layer optical thickness. For clarity, the matrix indices i and j are included in (11) and (12), and have the same meaning as in (9) and (10). The vector μ holds the viewing zenith angle cosines. The airmass factors in (11) and (12) are defined by

$$m_{ij} = \frac{1}{\mu_i} + \frac{1}{\mu_j} \quad \text{and} \tag{13}$$

$$n_{ij} = \frac{1}{\mu_j} - \frac{1}{\mu_i}. \tag{14}$$

For elements for which the incident and exiting directions are the same ($i = j$), $n_{ij} = 0$, and T_{ij} is computed from

$$T_{ij}^{\mathrm{ssi}} = e^{-\delta\tau/\mu_j}\left(E_{ij} + t_{ij}\frac{\delta\tau}{\mu_i}\right). \tag{15}$$

As pointed out by (Wiscombe 1975b), the most common initialization method used in adding/doubling methods is the infinitesimal generator initialization (IGI). The derivation of the IGI is given by Wiscombe (1975b); the resulting $\mathbf{R}_o$ and $\mathbf{T}_o$ initialization matrices are given by

$$R_{ij}^{\mathrm{igi}} = r_{ij}\frac{\delta\tau}{\mu_i} \quad \text{and} \tag{16}$$

$$T_{ij}^{\mathrm{igi}} = t_{ij}\frac{\delta\tau}{\mu_i} + E_{ij}\left(1 - \frac{\delta\tau}{\mu_i}\right). \tag{17}$$

As stated above, the goal here is obtain accuracy with as thick an initial layer as possible to reduce the number of doublings needed. One natural way to extend the accuracy of the IGI method for larger optical thicknesses is to replace the approximation for the exponential involving the slant-path optical depth in the IGI with the true exponential term. Once this approximation is made, the computation for the initial-layer quantities becomes

$$R_{ij}^{\mathrm{eigi}} = r_{ij}(1 - e^{-\delta\tau/\mu_i}) \quad \text{and} \tag{18}$$

$$T_{ij}^{\mathrm{eigi}} = t_{ij}(1 - e^{-\delta\tau/\mu_i}) + e^{-\delta\tau/\mu_j}E_{ij}. \tag{19}$$

To differentiate this method from the IGI, this method is referred to as the exponential infinitesimal generator initialization (EIGI).

One natural method to compute $\mathbf{Y}$, the layer emissivity, is to assume energy conservation such that

$$Y_i = 1 - \sum(R_{ij} + T_{ij}). \tag{20}$$

In physical terms, $\mathbf{Y}$ is the emissivity of the initial layer. Using (16) and (17) allows $\mathbf{Y}$ for the IGI to be computed as

$$Y_i^{\mathrm{igi}} = (1 - \tilde{\omega})\frac{\delta\tau}{\mu_i}, \tag{21}$$

which is also given in Wiscombe (1975a). For the EIGI, $\mathbf{Y}$ is computed as

$$Y_i^{\mathrm{eigi}} = (1 - \tilde{\omega})(1 - e^{-\delta\tau/\mu_i}). \tag{22}$$

Note that $\mathbf{Y}$ for the IGI and EIGI is the emissivity computed along direction i assuming no scattering. Although (21) can also be used to derive $\mathbf{Y}$ for the SSI, the emission that is scattered once in the layer can also be directly computed to give $\mathbf{Y}$ for the SSI as

$$Y_i^{\mathrm{ssi}} = (1 - \tilde{\omega}^2)(1 - e^{-\tau/\mu_i}) - (1 - \tilde{\omega})\sum_j (R_{ij}^{\mathrm{ssi}} + T_{s,ij}^{\mathrm{ssi}}). \tag{23}$$

The derivation of (23) is given in the appendix. Note that for the SSI, the **Y** derived from the single-scattering approximation [(20)] and by energy conservation [(23)] differ. As pointed out by Wiscombe (1975b), this implies that the SSI does not conserve energy. To derive a SSI that conserves energy while using the analytically derived expressions for **R**, **T**, and **Y**, we have chosen to modify the direction transmission term $\mathbf{T}_d$. Making this assumption in the direct transmission matrix using the SSI for the initial layer, $\mathbf{T}_d$ can be computed as

$$T_{d,ij}^{\mathrm{ssi}} = 1 - Y_i^{\mathrm{ssi}} - \sum_j (R_{ij}^{\mathrm{ssi}} + T_{s,ij}^{\mathrm{ssi}}), \tag{24}$$

where $T_{s,ij}^{\mathrm{ssi}}$ is the scattering transmission matrix for the initial layer given by (12) and (15) with the direct transmission component removed. Note that $\mathbf{T}_d^{\mathrm{ssi}}$ is the direct transmission term used only in the doubling initialization process. The actual value of $\mathbf{T}_d$ is used later in the iterative looping through the layers.

The last quantity needed to initialize the doubling sequence (**Z**) is initialized with a value of zero (Wiscombe 1975a). The term g_h in (7) is initialized with a value of $(\delta\tau)/2$.

Accuracy of the initialization methods for single-layer computations

This section explores the accuracy of the initialization methods in determining the final radiative properties of single model layers. For these simulations, the SOI model was run in its default configuration, which is the 4 + 2–stream model, with a maximum initial-layer optical thickness of 0.01. The additional stream was arbitrarily placed at $\mu = 0.866$ for these computations.

The errors shown in this section are the mean root-mean-square differences over all matrix elements between the true values along each direction and those predicted for a particular initialization scheme. For example, the errors in reflectance matrix predicted using the SSI, ϵ_{SSI}, are computed as

$$\epsilon^{\mathrm{ssi}} = \left[\frac{\sum (R_{ij}^{\mathrm{ssi}} - R_{ij}^{\mathrm{true}})^2}{n_s}\right]^{1/2}, \tag{25}$$

where n_s is the total number of elements in the reflectance matrices. The truth values used in computing these errors were generated using a full doubling procedure, accomplished by using the full matrix inversion for the computation of $\mathbf{\Gamma}$ and using the EIGI initialization with a very small initial-layer thickness $O(10^{-6})$.

The errors in final-layer reflection matrices computed using (25) for the IGI, EIGI, and SSI initializations are given in Fig. 2. As with Fig. 1, the errors are plotted as a function of the single-scattering albedo $\tilde{\omega}$ and the layer optical depth τ. Also shown in the lower-right-hand plot in Fig. 2 are the results for a hybrid initialization (HYB), which will be discussed later. In terms of the mean rms errors in **R**, the SSI is less accurate than IGI and EIGI for $\tilde{\omega} \geq 0.3$. In comparison with the IGI, the EIGI offers reduced errors in **R** for $\tau < \sim 0.2$. To avoid the patterns in the results caused by the discrete changes in the initial-layer optical thicknesses through the τ and $\tilde{\omega}$ domain, the results in Fig. 2, Fig. 3, and Fig. 4 have been spatially smoothed.

Figure 3 shows the rms errors in the scattering transmission matrices for single layers computed using (25) as a function of τ and $\tilde{\omega}$. The scattering transmission matrix $\mathbf{T}_s$ is defined as

$$T_{s,ij} = T_{ij} - e^{-\tau/\mu(j)}\delta_{ij}. \tag{26}$$

As was the case with Fig. 2, Fig. 3 shows that the SSI offers the largest scattering transmission matrix errors for larger τ and larger $\tilde{\omega}$. However, the $\tau - \tilde{\omega}$ region where the SSI offers smaller errors than the IGI and EIGI methods is larger and extends for all $\tilde{\omega} < \sim 0.6$, for all values of τ.

The rms errors computed using (25) for the upwelling source vector $\mathbf{S}^+$ are given in Fig. 4. One obvious feature of Fig. 4 is that both the SSI and IGI results have large errors (>5%) in different regions of the $\tau - \tilde{\omega}$ space. The SSI performed worse for large values of τ and $\tilde{\omega}$, and the IGI performed worse for low values of τ and $\tilde{\omega}$. In contrast, the EIGI initialization errors never exceed 5% for any value of τ or $\tilde{\omega}$.

As will be demonstrated in Part II, the primary application of the SOI model is the simulation of microwave radiances. However, there was no single initialization method that resulted in the most accurate **R**, $\mathbf{T}_s$, and $\mathbf{S}^{\pm}$ for all values of $\tilde{\omega}$ and τ. To illustrate this, Fig. 5 graphically shows the regions where each of the individual initializations (IGI, SST, and EIGI) gave the most accurate values of **R**, $\mathbf{T}_s$, and $\mathbf{S}^{\pm}$. As Fig. 5 shows, the SSI is superior in terms of the accuracy of **R** and $\mathbf{T}_s$ for $\tilde{\omega} < 0.5$. For computing **R** for values of $\tilde{\omega} > \sim 0.5$, the EIGI is more accurate relative to the IGI for $\tau < \sim 1$. For computing $\mathbf{T}_s$ for values of $\tilde{\omega} > \sim 0.5$, the EIGI is superior to the IGI for all values of τ. When computing $\mathbf{S}^{\pm}$, the SSI is generally the most accurate, except for values of $\tau > \sim 0.2$ and $\tilde{\omega} > \sim 0.6$ where the IGI and

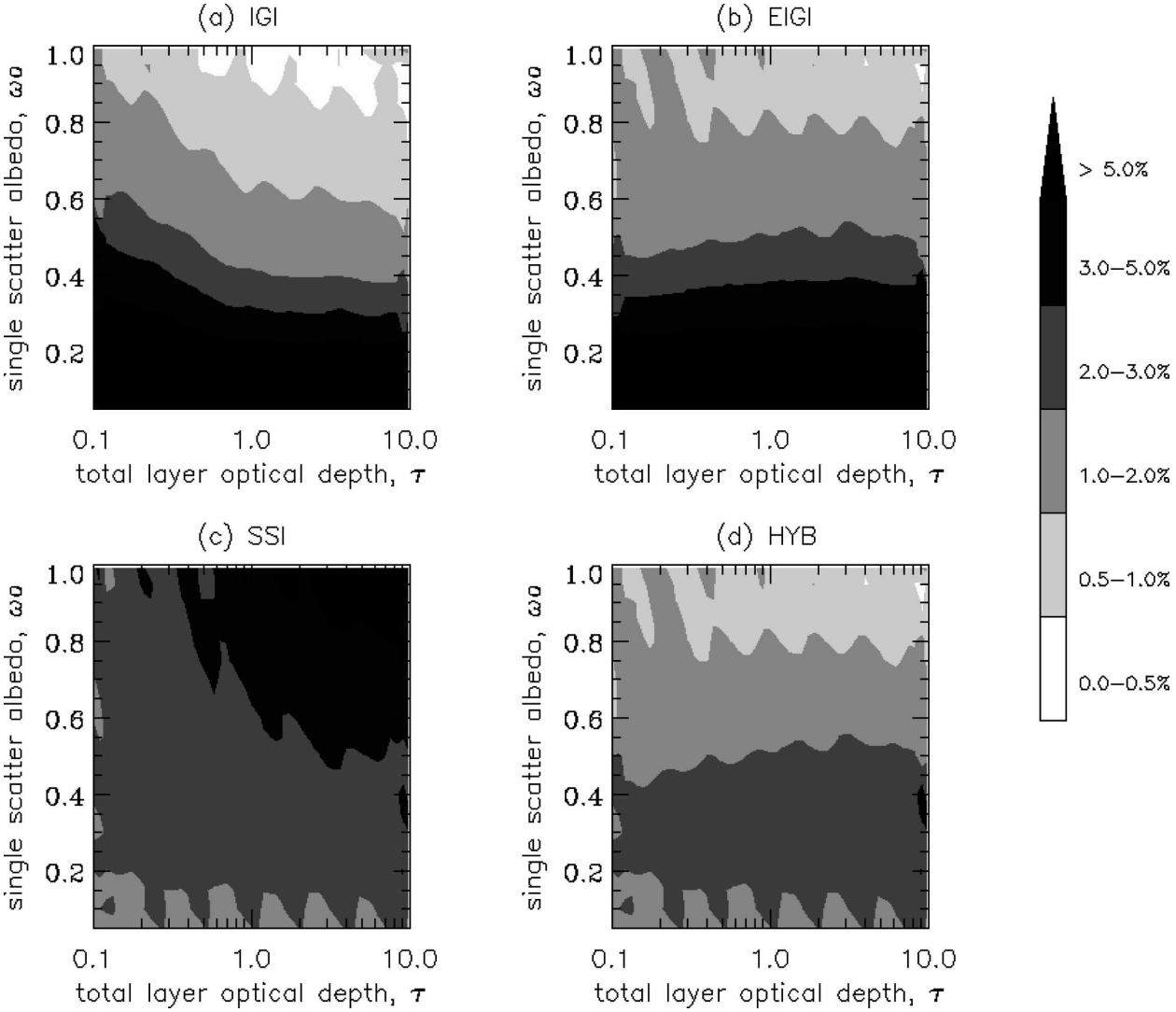

FIG. 2. Mean rms errors expressed as percentage of the single-layer reflectance matrix elements as a function of layer optical thickness and single-scattering albedo using the (a) IGI, (b) EIGI, (c) SSI, and (d) HYB initializations.

EIGI produce more accurate values. One method to overcome these shortcomings of the individual initialization methods is to use an HYB initialization method that is a combination of the different methods. In this analysis, the HYB method was chosen such that the EIGI method was used for $\tilde{\omega} > 0.6$ and the SSI for $\tilde{\omega} < 0.6$. As the results in Figs. 2–4 indicate, the HYB approach appears to offer a superior initialization in terms of the rms errors in $\mathbf{R}$, $\mathbf{T}_s$, and $\mathbf{S}^{\pm}$ for single layers.

In conclusion, it appears the SSI initialization is inferior to the EIGI initialization for computing the single-layer properties for $\tilde{\omega} > \sim 0.6$. This result is similar to that reported by Wiscombe (1975b), where he reported on the inferiority of the SSI to IGI initialization approach. The HYB approach appears to offer the best performance over the widest range of scattering conditions.

c. *Vertical integration*

In a traditional adding/doubling model, the computation of the radiances exiting an atmosphere composed of multiple layers involves the method of adding. Adding two layers is computationally similar to a doubling step except that the layers are not required to be identical. Because adding is applied to whole and combinations of whole layers, a similar truncation used in the doubling is not practical unless the layers are optically thin. In addition, the adding method requires matrix inversions, which can be computationally expensive.

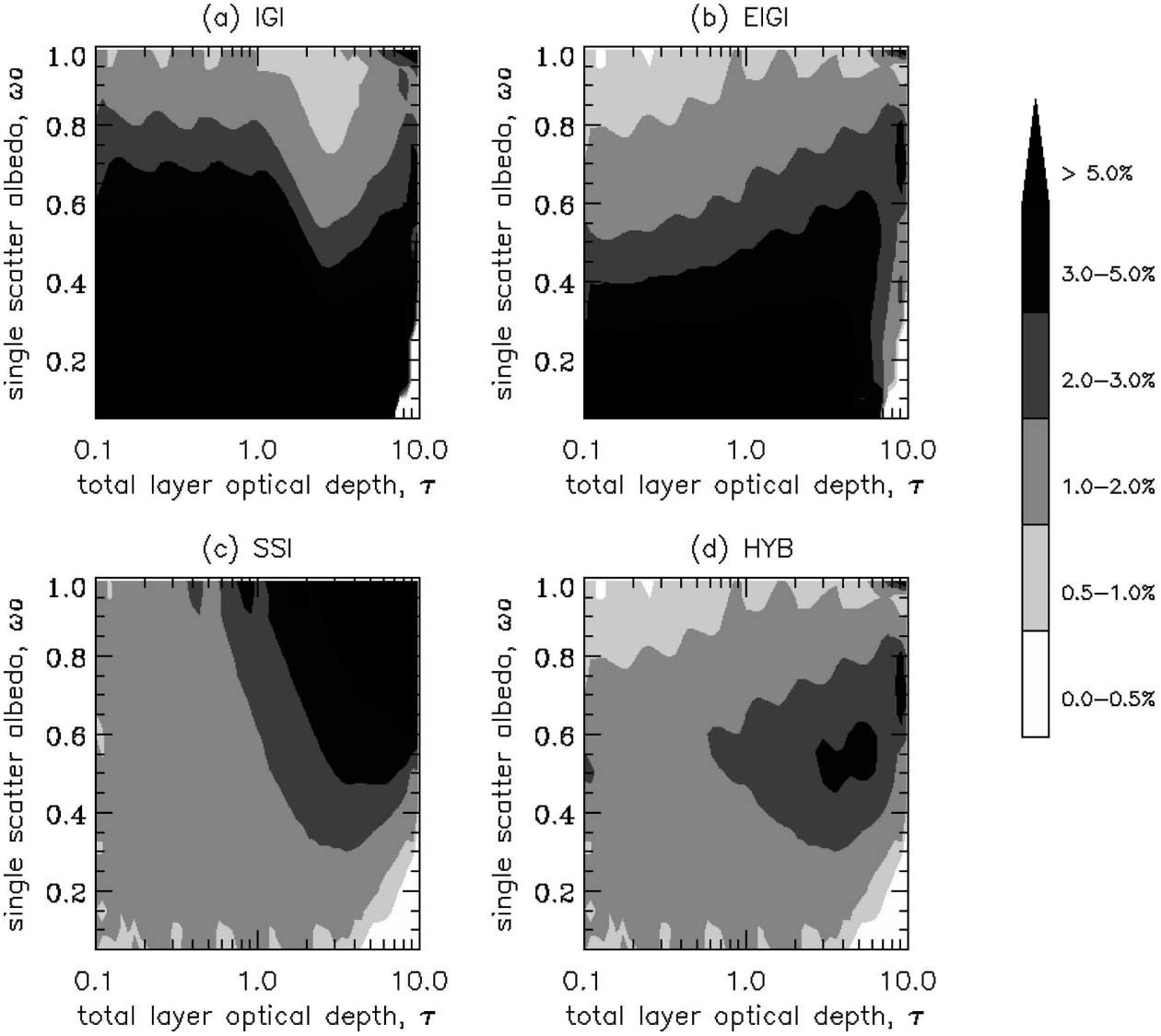

FIG. 3. Mean rms errors expressed as a percentage of the single-layer scattering transmission matrix elements as a function of layer optical thickness and single-scattering albedo using the (a) IGI, (b) EIGI, (c) SSI, and (d) HYB initializations.

To combine the atmospheric layers to derive the radiance incident on the satellite, we apply an approach similar to that used in the SOS model described by Greenwald et al. (2005). This method replaces the adding method with an iterative procedure, where the total radiance exiting the atmosphere is computed successively for each "order of interaction." This involves looping through the layers and computing the interaction of radiation from the previous order of interaction with each layer.

The process is begun by initializing the zeroth-order upwelling radiance at the surface as

$$\mathbf{I}_0^+(n) = e_{\text{sfc}} B_{\text{sfc}}, \tag{27}$$

where e_{sfc} is the surface emissivity and B_{sfc} is the emission of a blackbody at the temperature of the surface. The zeroth-order upwelling radiance (or brightness temperature) at level l [$\mathbf{I}_0^+(l)$] is computed as

$$\mathbf{I}_0^+(l) = \mathbf{S}^+(l) + \mathbf{T}_d(l)\mathbf{I}_0^+(l+1), \tag{28}$$

where $\mathbf{T}_d(l)$ is the direct transmission for the layer below l and $\mathbf{I}_0^+(l+1)$ is the zeroth-order radiance upwelling at level $l+1$. In this example, level 1 is the top of the atmosphere and the level index increases as one moves down through the atmosphere.

The zeroth-order downwelling radiance at the top of the atmosphere is initialized with the space emission term,

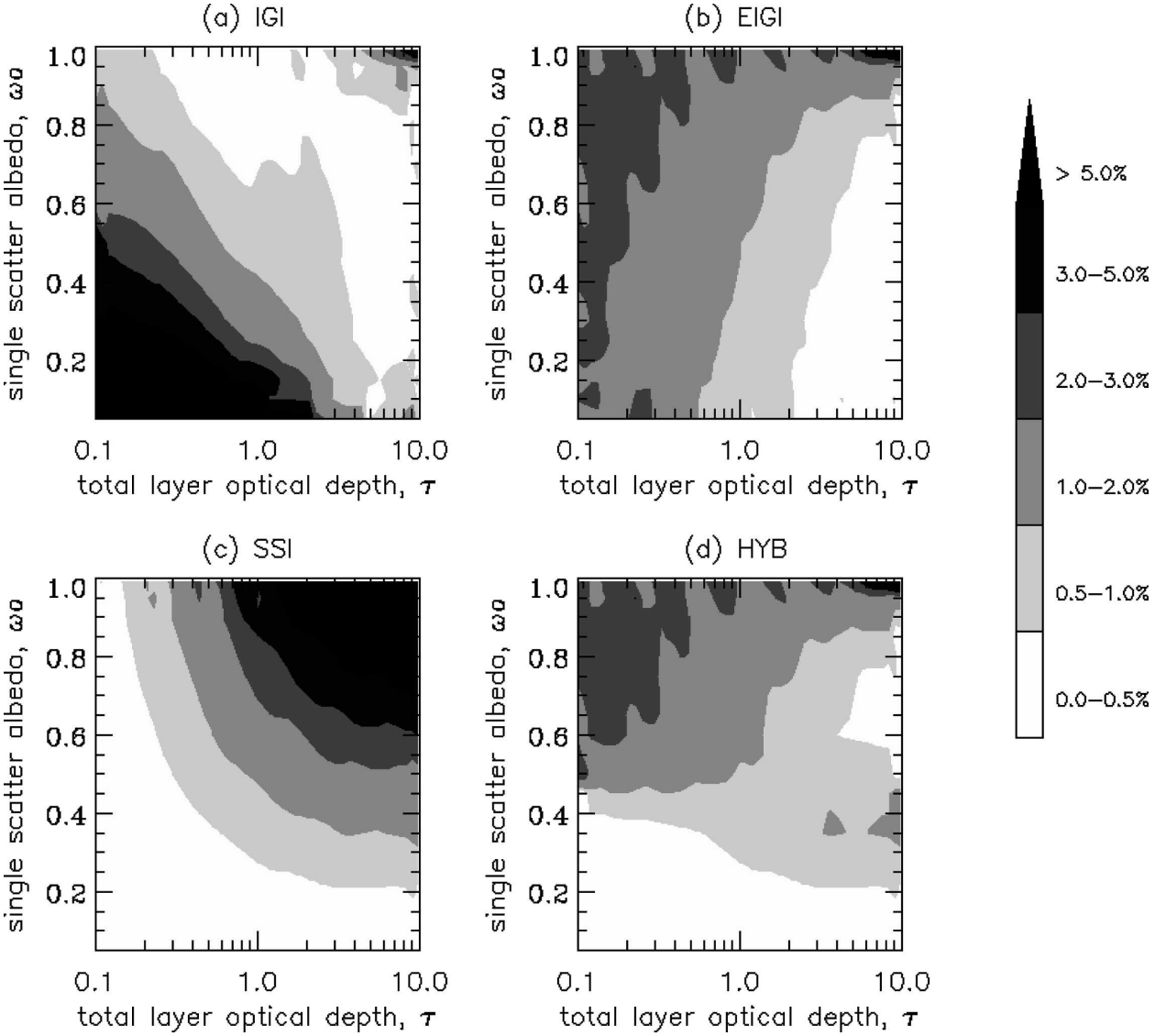

FIG. 4. Mean rms errors expressed as a percentage of the upwelling source vector elements $\mathbf{S}^+$ as a function of layer optical thickness and single-scattering albedo using the (a) IGI, (b) EIGI, (c) SSI, and (d) HYB initializations.

$$\mathbf{I}_0^-(1) = B_{\text{space}}. \tag{29}$$

The zeroth-order downwelling radiance is computed by moving down through the atmosphere, and the downwelling radiance at level l [$\mathbf{I}_0^-(l)$] is computed as

$$\mathbf{I}_0^-(l) = \mathbf{S}^-(l-1) + \mathbf{T}_d(l-1)\mathbf{I}_0^-(l-1), \tag{30}$$

where $\mathbf{T}_d(l-1)$ is the direct transmission for the layer above $l-1$ and $\mathbf{I}_0^-(l-1)$ is the downwelling zeroth-order radiance at level $l-1$.

The upwelling radiance at the surface for the next order of interaction k is the reflection off the lower surface (at level n) of the downwelling radiance of the previous order of interaction $k-1$,

$$\mathbf{I}_k^+(n) = (1 - e_{\text{sfc}}) \times \mathbf{I}_{k-1}^-(n). \tag{31}$$

The upwelling radiance at level l for the kth order of interaction is computed using the following relation:

$$\mathbf{I}_k^+(l) = \mathbf{R}(l)\mathbf{I}_{k-1}^-(l) + \mathbf{T}_s(l)\mathbf{I}_{k-1}^+(l+1) + \mathbf{T}_d(l)\mathbf{I}_k^+(l+1), \tag{32}$$

where $\mathbf{R}(l)$, $\mathbf{T}_s(l)$, and $\mathbf{T}_d(l)$ are, respectively, the reflection, scattering transmission, and direct transmission matrices for layer l. Here $\mathbf{I}_k^+(l)$ [$\mathbf{I}_k^-(l)$] is the upwelling (downwelling) radiance at level l in the kth order of interaction. This computation is initiated at the level of the surface and progresses upward through the atmosphere.

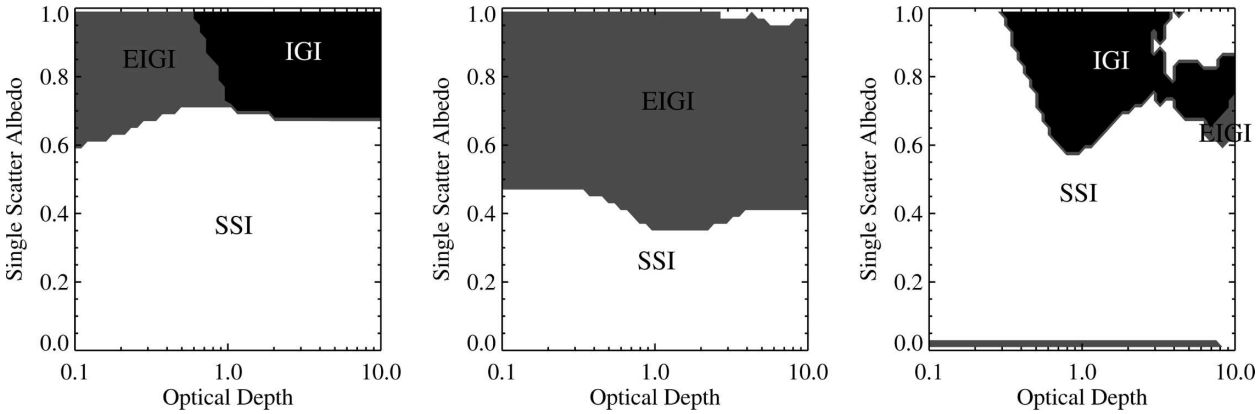

FIG. 5. Regions in the optical depth τ and single-scattering albedo $\tilde{\omega}$ domain where each of the three initializations (IGI, SSI, and EIGI) is most accurate. The results are shown for computing (left) $\mathbf{R}$, (middle) $\mathbf{T}_s$, and (right) $\mathbf{S}^{\pm}$.

Using the same conventions as in (32), the downwelling radiance at level l for the kth order of interaction is computed using the following relation:

$$\mathbf{I}_k^-(l) = \mathbf{R}(l-1)\mathbf{T}_{k-1}^+(l) + \mathbf{T}_s(l-1)\mathbf{I}_{k-1}^-(l-1) + \mathbf{T}_d(l-1)\mathbf{I}_k^-(l-1). \quad (33)$$

This computation is started at the first level and progressed downward to the surface.

ACCELERATION OF THE CONVERGENCE

The scheme outlined above for computing the radiance contribution for each order of interaction is iterated until sufficient accuracy is achieved. One method of achieving convergence is to increase the orders of interaction until the contribution of each order of interaction is less than some threshold. For example, Fig. 6 shows the convergence of the top-of-atmosphere radiance as a function of the order of interaction. The curve labeled "unaccelerated" represents the simple sum of all of the previous orders of interaction. This simulation is for a surface with an emissivity of 0.4 and a temperature of 300 K. The atmosphere is assumed to be isothermal with a temperature of 285 K. In addition, the atmosphere was assumed to be composed of 10 identical layers. The EIGI initialization and single-term truncated doubling were used to generate the properties of each layer. The curves show the results for two sets of cloud properties. The model was run in the 4 + 2–stream configuration with an observation angle of 30°. For these simulations, it was assumed that convergence was achieved when the radiance contribution for an order of interaction was less than 0.1 K. For the optically thick and low-absorption case ($\tau = 10$; $\tilde{\omega} = 0.9$) this was achieved after simulating 25 orders of interaction. For the optically thinner and more-absorbing case ($\tau = 1$; $\tilde{\omega} = 0.5$), the convergence occurred after eight orders of interaction.

As is common in Monte Carlo radiative transfer schemes, the convergence of the series of orders of scattering can be accelerated. Our goal here is to demonstrate that this approach can be applied to the SOI model so that its range of applicability can be extended into atmospheres with higher amounts of scattering. This particular acceleration method was briefly described by Greenwald et al. (2005) and was derived by Heidinger (1997) for use in a backward Monte Carlo model. The basic assumption of the acceleration technique is that for higher orders of scattering the ratio of the contribution to the total radiance from the current order and the next order of scatter is a constant (Irvine 1964). Making this assumption, a method of acceleration can be derived as follows:

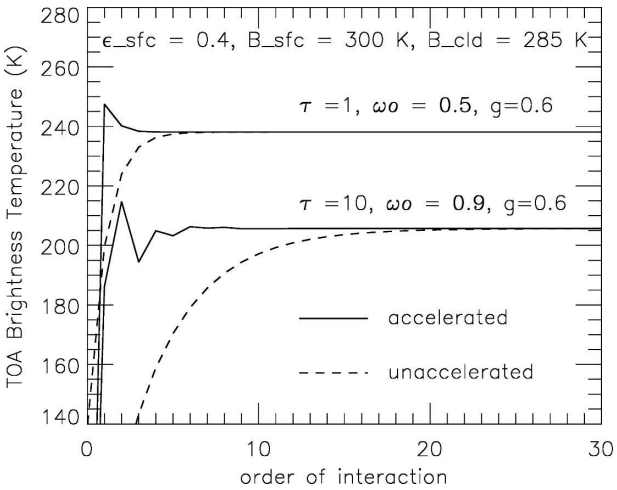

FIG. 6. Convergence of the top-of-atmosphere brightness temperature for two cases.

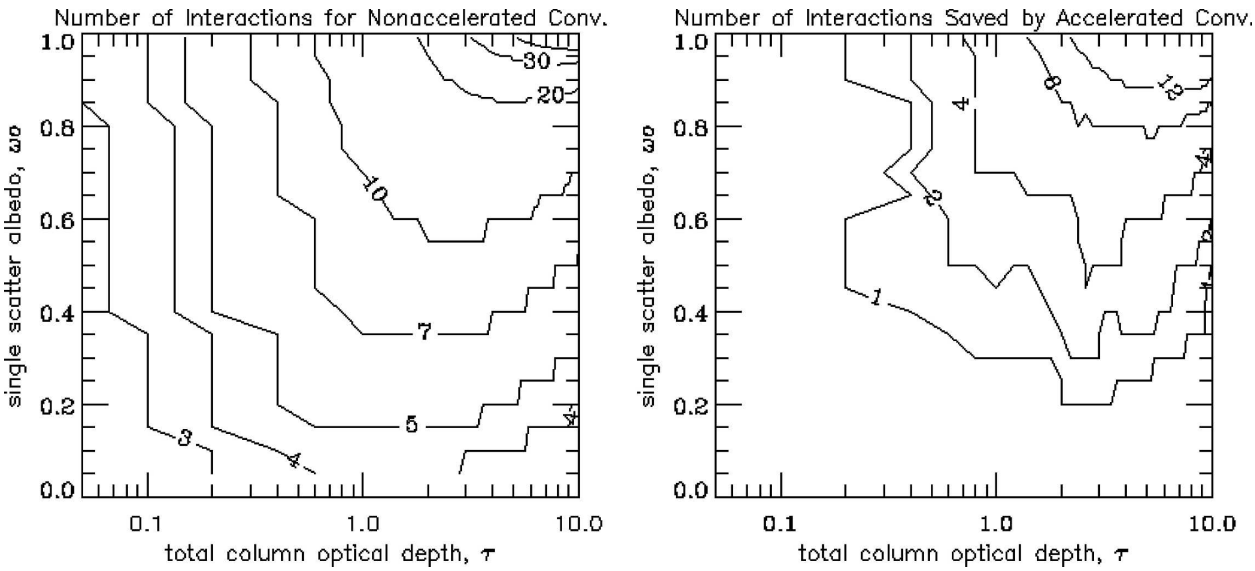

FIG. 7. Numbers of interactions required for convergence.

$$\mathbf{Q}_k = \mathbf{S}_k + \frac{(\mathbf{I}_k)^2}{(\mathbf{I}_{k-1} - \mathbf{I}_k)}, \tag{34}$$

where $\mathbf{I}_k$ is the radiance contribution from the kth order of interaction, $\mathbf{S}_k$ is the sum of the radiance from all orders of interaction less than or equal to k, and $\mathbf{Q}_k$ is the estimate of the final value of the converged series after k interactions.

Figure 6 shows results using this method of acceleration applied to the simulations described above. The results indicate that this acceleration technique holds promise for reducing the required orders of interaction for optically thick and highly scattering atmospheres. The accelerated series was considered converged if two consecutive terms of $\mathbf{Q}$ did not change by a value that was 2 times the value used to test the unaccelerated series for convergence. The accelerated convergence threshold was 2 times the unaccelerated convergence threshold because the accelerated series may overestimate or underestimate the final answer whereas the unaccelerated series always underestimates the final answer. Note that for low orders of interaction the estimate of $\mathbf{Q}_k$ is not monotonic. For this reason, the convergence requires that the convergence criterion be met for two consecutive orders of interaction.

The convergence results for a wide range of optical properties are given in Fig. 7. The simulation conditions in Fig. 7 are identical to those in Fig. 6. The contours in Fig. 7 show the order of interaction required for convergence. The plot on the left shows the results for the unaccelerated series, and the plot on the right gives the reduction in the number of interactions needed for convergence using the above acceleration technique.

In general, the radiance series converges for a few orders of interaction for $\tau < \sim 1$ for all values of $\tilde{\omega}$. For optically thick and less-absorbing atmospheres, many more orders of interaction are needed, and values exceeding 30 orders of interaction are required when $\tilde{\omega} \geq 0.9$ and $\tau \geq 4$. In summary, when using the series acceleration, the number of orders of interaction required for convergence is greatly reduced for optically thick and strongly scattering atmospheres.

d. Treatment of polarization

It is important to note that the SOI model developed here neglects polarization in the atmosphere, in that it adopts an intensity-only phase function. However, in the application of the SOI for microwave simulations, polarization can be and is generated at the surface through unequal surface emissivity in the two polarization states V and H; thus, the SOI model returns both top-of-atmosphere brightness temperatures $\mathbf{T}_{b,v}$ and $\mathbf{T}_{b,h}$. The assumption is that if a photon scatters off a layer (either forward or backward), any polarization information is erased. The reasoning behind this assumption is that, in the azimuth average, polarization is greatly reduced when it is averaged over the 360° of azimuthal direction. However, it is most certainly an assumption and may not always be suitable, depending on the situation. For the results in this paper, the effects of a polarizing surface are ignored. The assumptions in the SOI model described above do not prohibit the inclusion of polarization. For example, Herman et al. (1995) describe the inclusion of polarization into a model that uses an iterative approach similar to that of the SOI model.

3. Application to simulation of satellite microwave observations

The previous sections have described the potential benefits of the SOI method. The results shown earlier were confined to simulations of single isothermal layers or multiple but identical isothermal layers. The accuracy of the SOI model for a given initialization scheme is governed by two parameters: the number of quadrature abscissas or streams n_s, and the initial-layer optical thickness $\delta\tau$. In this section, values of these parameters that are optimal for the simulation of microwave observations are determined. This model using these values will serve as the basis for the more rigorous application of the SOI model in Part II.

To determine the values of n_s and $\delta\tau$, comparisons were made between the SOI model and a Monte Carlo model (Petty 1994). In these simulations, the SOI model was run using the HYB initialization. The atmospheric profiles used for this comparison were taken from Smith et al. (2002). The four cases used in Smith et al. represent different states of cloud and precipitation. In this analysis, only results from case 4 are shown, which represents the most challenging profile to the SOI model because it contains high ice and water contents with a rain rate of 90.23 mm h^{-1}. The Monte Carlo model simulations were generated using sufficient numbers of photon trajectories to ensure that the uncertainties were below 0.1 K for all frequencies. The frequencies used for this analysis, the same as used in Smith et al., are 10.7, 19.4, 37.0, and 85.5 GHz. The amount of scattering and hence the computational difficulty generally increases with each of the above frequencies such that the most difficult simulation is for 85.5 GHz. Smith et al. compared observations at zenith angles of 0° and 53.1°, but we will restrict this analysis to simulating radiances at 53.1°. The performance of the SOI model for a wide range of observation angles will be described in Part II.

As stated above, the goal here is to select optimal values of n_s and $\delta\tau$ for the SOI model. By optimal, it is meant that the chosen values minimize the computational burden while maintaining sufficient accuracy. For cases in which the total scattering optical depth is less than 0.01, a 2 + 2–stream model with $\delta\tau = 0.1$ was found to be sufficient to maintain errors of less than ~0.2 K for the relevant cases and frequencies from Smith et al. (2002). When the total scattering optical depth exceeded 0.01, it was found that more streams were needed. For example, Fig. 8 shows the errors in the SOI model for case 4 relative to the Monte Carlo model as function of the number of streams used in the simulation n_s. In this figure, n_s refers to the total number of streams per hemisphere, excluding the additional stream placed at the observation angle. For this simulation, the value of $\delta\tau$ was set to a value (0.0001) small enough to ensure that the final error was dominated by the choice of n_s, not $\delta\tau$. As the figure shows, errors for frequencies for case 4 fall below 1 K for n_s larger than or equal to 4. Although there is a slight improvement in the results for increasing the number of streams beyond 4, the increase in accuracy is not warranted, given the other uncertainties in radiative transfer modeling. Therefore, a value of n_s of 4 appears to be optimal for simulating microwave observations with the SOI method.

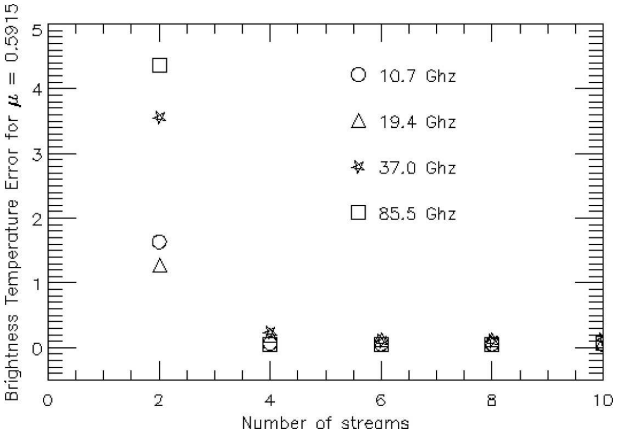

FIG. 8. SOI model error as a function of number of streams (excluding the observation stream).

Figure 9 shows the variation of the SOI errors relative to the Monte Carlo model as function of $\delta\tau$ for the value of n_s chosen above ($n_s = 4$). In the ideal case, the magnitude of the errors resulting from each parameter should be equivalent. There is little need to specify a small value of $\delta\tau$ if the error resulting from the approximation of the radiance field by the n_s streams is the dominant error source. From Fig. 8, the mean errors in the 4 + 2–stream SOI model with a small value of $\delta\tau$ were all less than 0.2 K for case 4. The largest error for any cases or frequency combination was 0.48 K. Therefore, an optimal value of $\delta\tau$ would be one that produces a similar error. From Fig. 9, it is apparent the errors begin to exceed 0.5 K for $\delta\tau > \sim 0.01$ for the case-4 simulations. Based on the case-4 comparisons, the optimal value of $\delta\tau$ for the SOI model is therefore roughly 0.01 for simulating the case-4 results.

In summary, these comparisons with the Monte Carlo model indicate that the optimal configuration of the SOI model is a 4 + 2–stream model with $\delta\tau < \sim 0.01$. The absolute accuracy of the SOI model over a wide range of realistic conditions will be explored in Part II, but it is important to note the overall accuracy

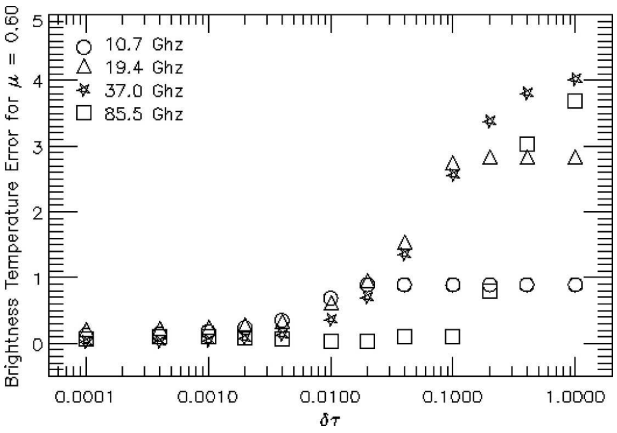

FIG. 9. SOI model error, using 4 + 2 streams, as a function of initial-layer thickness.

of the SOI model in simulating the atmospheric profiles and frequencies for the Smith et al. (2002) cases. When compared with the spread of results from the models included in the original comparisons of Smith et al., the SOI model fares well, especially relative to some two-stream models, which have difficulty modeling the angular variation of observations for some case/frequency combinations. Part II will fully demonstrate the benefits of the SOI model using more realistic simulations.

4. Conclusions

This study has demonstrated that the SOI method offers an accurate and computationally efficient solution for azimuthally symmetric radiative transfer. Part II will demonstrate that these computational benefits are sufficient to allow the SOI method to be used in microwave radiance assimilation schemes.

The analysis shown here indicates that the approximations used in developing the SOI method are valid for a wide range of applications in the microwave and infrared spectral regions. For example, the truncation of the doubling method using a one- or two-term expansion was shown to be accurate for scattering layers typical of those in the infrared and microwave regions. In addition, the number of interactions needed to achieve convergence is typically less than 5 for most atmospheric profiles. When large amounts of scattering require it, a method for the acceleration of the convergence of the results was demonstrated. An extension of the infinitesimal generator initialization method was found to offer the best performance for any one initialization method. A hybrid initialization method was developed based on a combination of the EIGI and SSI methods that appears to offer superior performance for the cases simulated.

A comparison of the SOI model versus a full Monte Carlo model using the atmospheric profiles given by Smith et al. (2002) was used to determine the optimal parameters for the SOI implementation. For the simulation of microwave top-of-atmosphere radiances, this analysis indicated that the optimal number of streams n_s was 4 and that of the initial-layer optical thickness limit $\delta\tau$ was 0.01.

In Part II, the accuracy and applicability of the SOI method of radiative transfer will be demonstrated. Part II will show that the SOI model is an accurate and efficient method for simulating microwave radiances for most atmospheric conditions and is often superior in accuracy to the standard two-stream approaches for a comparable computational burden. Last, Part II will demonstrate the application of this model and its adjoint for microwave radiance assimilation studies. Additional work is being directed toward applying the SOI method for infrared satellite radiance simulations.

Acknowledgments. This work was funded by the Joint Center for Satellite Data Assimilation (JCSDA) through NOAA Cooperative Agreement NA07EC0676 and the NOAA Office of Research and Applications. The views, opinions, and findings contained in this report are those of the author(s) and should not be construed as an official National Oceanic and Atmospheric Administration or U.S. government position, policy, or decision.

APPENDIX

Derivation of the Single-Scattering Source

Equation (23) can be derived as follows. Consider a layer of uniform temperature T, optical thickness τ, and single-scattering albedo $\tilde{\omega}$. Radiation emitted from an arbitrary location within the layer has multiple possible fates: it can make it out directly (without scattering), it can be scattered yet still emerge from the layer, or it can be absorbed at some other location within the layer. An expression for the portion of thermal radiation emitted from the layer, without scattering, into a zenith angle with cosine μ is easily derived and is given by

$$\mathbf{l}_0(\mu) = \mathbf{Y}_0(\mu)B(T) = (1 - \tilde{\omega})(1 - e^{-\tau/\mu})B(T), \tag{A1}$$

where $B(T)$ is the Planck function at temperature T, and $\mathbf{Y}_0$ is the emissivity of the layer under the no-scattering assumption. However, (A1) misses all of the thermal radiation scattered within the layer yet still making it out. We can refine our expression for the layer thermal source by calculating that portion of the

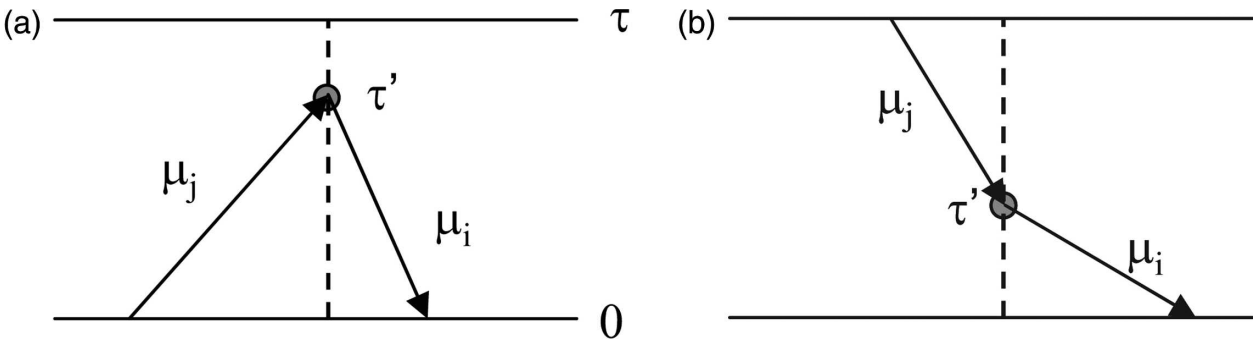

FIG. A1. Example of thermal radiation emitted within a layer and subsequently scattered once into either the (a) backward or (b) forward direction. The contribution from all such scattering locations τ' is obtained by a straightforward integration.

thermal radiation scattered exactly once; let this portion be given by $\mathbf{l}_1(\mu) = \mathbf{Y}_1(\mu)B(T)$.

We now present a simple derivation for $\mathbf{Y}_1$ under the assumption of Gaussian quadrature. Consider Fig. A1a. Thermal radiation emitted along the angle μ_j is backscattered at the location τ', and some fraction of it is scattered into the angle μ_i. By regarding the location of scattering as an infinitesimal layer surrounding τ', with optical thickness $d\tau'$ and single-scattering albedo $\tilde{\omega}$, the fraction of radiation backscattered from μ_j to μ_i is given by

$$\mathbf{R}^{\mathrm{igi}}(i,j) = \frac{\tilde{\omega}d\tau'}{2\mu_i}\mathbf{P}^-(i,j)w_j, \tag{A2}$$

where w_j is the quadrature weight associated with stream j, and the usual normalization condition

$$\sum_j [\mathbf{P}^+(i,j) + \mathbf{P}^-(i,j)]w_j = 2 \tag{A3}$$

is assumed. The singly backward-scattered thermal radiation, emitted along stream j and scattered into stream i at location τ', is then given by

$$\mathbf{S}_1^-(i,j,\tau') = [(1-\tilde{\omega})(1-e^{-\tau'/\mu})B(T)]\mathbf{R}^{\mathrm{igi}}(i,j)e^{-\tau'/\mu_i}. \tag{A4}$$

Integrating this over the layer optical thickness, it is straightforward to show that the thermal contribution from singly backward-scattered radiation, emitted along stream j and scattered into stream i, is given by

$$\mathbf{S}_1^-(i,j) = B(T)(1-\tilde{\omega})[(\tilde{\omega}/2)(1-e^{-\tau/\mu_i})\mathbf{P}^-(i,j) - \mathbf{R}^{\mathrm{ssi}}(i,j)], \tag{A5}$$

where $\mathbf{R}^{\mathrm{ssi}}$ is the reflection matrix of the full layer under the single-scattering assumption, given by (11). In a similar way, the contribution from singly forward-scattered radiation (Fig. A1b) can be shown to be

$$\mathbf{S}_1^+(i,j) = B(T)(1-\tilde{\omega})[(\tilde{\omega}/2)(1-e^{-\tau/\mu_i})\mathbf{P}^+(i,j) - \mathbf{T}_s^{\mathrm{ssi}}(i,j)], \tag{A6}$$

where $\mathbf{T}_s^{\mathrm{ssi}}$ is the forward-scattered-transmission matrix under the single-scattering assumption [(12)]. Summing over all streams j, and employing the phase function normalization condition [(37)], we obtain

$$\mathbf{Y}_1(\mu_i) = \frac{1}{B(T)}\sum_j [\mathbf{S}_1^-(i,j) + \mathbf{S}_1^+(i,j)] = \tilde{\omega}(1-\tilde{\omega}) \times (1-e^{-\tau/\mu_i}) - (1-\tilde{\omega})\sum_j [\mathbf{R}^{\mathrm{ssi}}(i,j) + \mathbf{T}_s^{\mathrm{ssi}}(i,j)]. \tag{A7}$$

Adding this to the contribution from the unscattered thermal radiation $\mathbf{Y}_0(\mu_i)$ yields the thermal source emissivity under the single-scattering assumption,

$$\mathbf{Y}(\mu_i) = (1-\tilde{\omega}^2)(1-e^{-\tau/\mu_i}) - (1-\tilde{\omega})\sum_j [\mathbf{R}^{\mathrm{ssi}}(i,j) + \mathbf{T}_s^{\mathrm{ssi}}(i,j)]. \tag{A8}$$

REFERENCES

Bauer, P., P. Lopez, A. Benedetti, E. Moreau, D. Salmond, and M. Bonazzola, 2004: Assimilation of satellite-derived precipitation information at ECMWF in preparation of a future European contribution to GPM (EGPM). ECWMF Internal Rep. 17193, 85 pp.

Busbridge, I. W., 1960: *The Mathematics of Radiative Transfer*. Cambridge University Press, 143 pp.

Evans, K. F., and G. L. Stephens, 1990: Polarized radiative transfer modelling: An application to microwave remote sensing of precipitation. Department of Atmospheric Science, Colorado State University Atmospheric Science Blue Book 461, 79 pp.

Greenwald, T., R. Bennartz, C. W. O'Dell, and A. Heidinger, 2005: Fast computation of microwave radiances for data assimilation using the "successive order of scattering approximation." *J. Appl. Meteor.,* **44,** 960–966.

Hansen, J. E., 1969: Radiative transfer by doubling very thin layers. *Astrophys. J.,* **155,** 565–573.

Heidinger, A. K., 1997: Nadir sounding in the A-band of oxygen. Department of Atmospheric Science, Colorado State University Atmospheric Science Blue Book 650, 225 pp.

Herman, B. M., D. E. Flittner, T. R. Caudill, K. J. Thome, and A. Ben-David, 1995: Comparison of the Gauss-Seidel spherical polarized radiative transfer code with other radiative transfer codes. *Appl. Opt.,* **34,** 4563–4572.

Irvine, W. M., 1964: The formation of absorption bands and the distribution of photon optical paths in a scattering atmosphere. *Bull. Astron. Inst. Neth.,* **17,** 266–279.

——, 1965: Multiple scattering by large particles. *Astrophys. J.,* **142,** 1563–1575.

Liou, K. N., 2002: *An Introduction to Atmospheric Radiation*. Academic Press, 583 pp.

Liu, Q., and F. Weng, 2002: A microwave polarimetric two-stream radiative transfer model. *J. Atmos. Sci.,* **59,** 2396–2402.

O'Dell, C. W., A. K. Heidinger, T. Greenwald, P. Bauer, and R. Bennartz, 2006: The successive-order-of-interaction radiative transfer model. Part II: Model performance and applications. *J. Appl. Meteor. Climatol.,* **45,** 1403–1413.

Petty, G. W., 1994: Physical retrievals of over-ocean rain rate from multichannel microwave imagery. Part I: Theoretical characteristics of normalized polarization and scattering indices. *Meteor. Atmos. Phys.,* **54,** 89–100.

Smith, E. A., P. Bauer, F. S. Marzano, C. D. Kummerow, D. McKague, A. Mugnai, and G. Panegrossi, 2002: Intercomparison of microwave radiative transfer models for precipitating clouds. *IEEE Trans. Geosci. Remote Sens.,* **40,** 541–549.

Twomey, S., H. Jacobowitz, and H. B. Howell, 1966: Matrix methods for multiple-scattering problems. *J. Atmos. Sci.,* **23,** 289–298.

van de Hulst, H. C., and K. Grossman, 1968: Multiple light scattering in planetary atmospheres. *The Atmospheres of Venus and Mars,* J. C. Brand and M. B. McElroy, Eds., Gordon and Breach, 35–55.

Voronovich, A. G., A. J. Gasiewski, and B. L. Weber, 2004: A fast multistream scattering-based Jacobian for microwave radiance assimilation. *IEEE Trans. Geosci. Remote Sens.,* **42,** 1749–1761.

Weinman, J. A., and P. J. Guetter, 1977: Determination of rainfall distributions from microwave radiation measured by the *Nimbus 6* ESMR. *J. Appl. Meteor.,* **16,** 437–442.

Wendisch, M., and W. von Hoyningen-Huene, 1991: High speed version of the method of "successive order of scattering" and its application to remote sensing. *Beitr. Phys. Atmos.,* **64,** 83–91.

Wiscombe, W. J., 1975a: Extension of the doubling method to inhomogeneous sources. *J. Quant. Spectrosc. Radiat. Transfer,* **16,** 477–489.

——, 1975b: On initialization, error and flux conservation in the doubling method. *J. Quant. Spectrosc. Radiat. Transfer,* **16,** 637–658.